Scale Effects on Fire Properties of Materials

A. TEWARSON and J. S. NEWMAN
Factory Mutual Research Corporation
1151 Boston-Providence Turnpike
Norwood, Massachusetts 02062, USA

ABSTRACT

The scale effects on fire properties have been examined for materials in pool-like, box-like, and crib-like configurations.

For turbulent fires of a material, with varying sizes and geometrical arrangements, a chemical similarity was found for each specified value of ventilation and decomposition mode. The decomposition mode in the combustion of the material was found to be important for the production of CO and particulates.

I INTRODUCTION

Mathematical fire models are now available to evaluate the fire performance of materials in buildings and to estimate the hazards presented by such fires and required protection. Fire models require numerous input parameters, some related to materials and others related to environment. The input parameters are generally quantified in small-scale experiments; it is thus necessary that fire scale effects (if any) on the parameters be known and corrected accordingly.

Input parameters related to materials are needed by the models to describe: 1) fire initiation and growth; 2) mass flow of fuel vapors from the surface of the material; 3) generation of heat and chemical compounds; 4) light attenuation by particulates; 5) biological and corrosive effects of chemical compounds; and 6) efficiency of fire detection, suppression, and extinguishment.

In this paper, parameters describing the generation rates of heat and chemical compounds, and light attenuation by particulates have been considered.

II CONCEPTS

The concepts have been described in detail elsewhere[1-7]. As the fire scale changes, the mass flow rate of fuel vapors from the surface of the material and generation rates of heat and chemical compounds change. The parameters describing these rates, however, should be independent of the fire

scale, if fires are turbulent and the decomposition chemistry of the material remains invariant.

The total mass flow rate of the mixture of fire products and air, $\dot{m}_t$, can be expressed as:

$$\dot{m}_t = \dot{m}_a + \dot{m}_f \quad , \tag{1}$$

where $\dot{m}_a$ = mass flow rate of air (g/s); and $\dot{m}_f$ = mass flow rate of fuel vapors (g/s). If we express the ratio between $\dot{m}_f$ and $\dot{m}_t$ as X_f, then the following relationships can be derived for the generation rates of heat and chemical compounds:

$$\dot{G}_j = X_j \dot{m}_t = Y_j X_f \dot{m}_t \quad , \tag{2}$$

$$\dot{Q}_A = (H_T/k_j) X_j \dot{m}_t = (H_T/k_j) Y_j X_f \dot{m}_t \quad , \tag{3}$$

and,

$$\dot{Q}_C = \chi_C H_T X_f \dot{m}_t = \Delta T c_p \dot{m}_t \quad , \tag{4}$$

where, $\dot{G}_j$ = mass generation of a chemical compound (g/s); X_j = mass fraction of the compound (g/g); Y_j = mass of the compound generated per unit mass of the fuel vapors defined as the yield of the chemical compound (g/g); $\dot{Q}_A$ = generation rate of heat associated with chemical reactions in the fire, defined as the actual heat release rate (kW); in Eq (3), compound j is associated with complete combustion; H_T = net theoretical heat of complete combustion per unit mass of the fuel vapors (kJ/g); k_j = maximum possible theoretical yield of the compound (g/g); $\dot{Q}_C$ = convective heat release rate (kW); χ_C = convective component of combustion efficiency; and c_p = average specific heat of the mixture of fire products and air at the gas temperature (kJ/g K).

The theoretical heat release rate, $\dot{Q}_T$, and the theoretical generation rate of a chemical, $\dot{G}_{Tj}$, can be expressed as

$$\dot{Q}_T = H_T X_f \dot{m}_t \quad . \tag{5}$$

$$\dot{G}_{Tj} = k_j X_f \dot{m}_t \quad . \tag{6}$$

The combustion efficiency, χ_A, is defined as the ratio between $\dot{Q}_A/\dot{Q}_T$, and the generation efficiency of a chemical compound, f_j, is defined as the ratio between $\dot{G}_j$ and $\dot{G}_{Tj}$. Thus

$$\chi_A = f_j = Y_j/k_j \quad . \tag{7}$$

Equation (7) implies that the ratios between various molecules of chemical compounds generated in the fire are conserved for various degrees of completeness of combustion. From Eqs (3) and (7):

$$\dot{Q}_A = H_T \chi_A X_f \dot{m}_t = H_T f_j X_f \dot{m}_t \quad . \tag{8}$$

In Eqs (4) and (8) $\chi_C H_T$ and $\chi_A H_T$ can be defined as convective and actual heat of combustion (H_C and H_A respectively). In a similar fashion, $\chi_R H_T$ can be defined as the radiative heat of combustion, H_R, where χ_R is the radiative component of the combustion efficiency.

The fraction of light attenuated by particulate, I/I_o, can be expressed as

$$D = \sigma_\lambda = \xi_\lambda X_S \rho_T = \xi_\lambda Y_S X_f \rho_T \ , \tag{9}$$

where $D = (1/\ell) \ln (I_O/I)$, defined as the optical density per unit path length ℓ; σ_λ = extinction coefficient of particulates (m^{-1}); ξ_λ = specific extinction coefficient of particulates (m^2/g); ρ_T = density of fire products and air (g/m^3); and λ = wave length of light (μ).

In order to examine the scale effects on the parameters, experiments can be performed at various fire scales and measurements made for $\dot{m}_f$, $\dot{G}_j$, $\dot{Q}_C$, and D. The accuracy of such an examination can be enhanced if the fire products and air, downstream of the reaction zone of the fire, are captured and are well mixed before the analytical measurements.

If the fire products and air are distributed nonuniformly and if heat losses and $\dot{m}_t$ values are unknown, such as in enclosure fires, then interrelationships between $\dot{m}_f$, $\dot{G}_j$, $\dot{Q}_C$, and D are needed for examining the scale effects.

2.1 Interrelationships Between Mass Flow Rate of Fuel Vapors, Generation Rates of Heat and Chemical Compounds, and Light Attenuation by Particulates

From Eqs (2), (4), and (7)

$$\Delta T/X_j = (1/c_p) (H_T/k_j) (\chi_C/f_j)$$

$$= (1/c_p) (H_T/k_j) (\chi_C/\chi_A) \ , \tag{10}$$

where j is a compound produced (or consumed) in those reactions where heat is also produced. For example, for oxygen f_O is defined as the depletion efficiency of oxygen.

From Eqs (2) and (9):

$$D/X_j = \xi_\lambda \rho_T (Y_S/Y_j) \ . \tag{11}$$

From Eqs (4) and (9):

$$\Delta T/D = (1/\xi_\lambda c_P \rho_T) (\chi_C/f_s) (H_T/k_s) \ . \tag{12}$$

In turbulent fires, $\Delta T/X_j$, D/X_j, and $\Delta T/D$ would be expected to be conserved from one location to another, because various ratios between H_T, χ_i, k_j, f_j, Y_j, Y_s, and ξ_λ are conserved. For turbulent fires, the radiative component of the combustion efficiency, χ_R, is also expected to be conserved.

In enclosure fires, ΔT, X_j, and D can be measured at various locations and the scale effects can be examined using Eqs (10) to (12), irrespective of mixing and dilution of the chemical compounds. However, in the analyses, it is necessary to differentiate between effects related to fire scale, to fire chemistry, and to heat losses.

2.2 Factors Affecting the Mass Flow Rate of Fuel Vapors, Generation of Heat and Chemical Compounds, and Light Attenuation by Particulates

2.2.1 Fire Scale. Fire scale affects the mass flow rate of fuel vapors from the surface of the material, due to variations in the flame radiative heat flux, $\dot{q}''_{fr}$. As fire scale increases, $\dot{q}''_{fr}$ and the corresponding value of the mass flow rate of fuel vapors per unit surface area of the material, $\dot{m}''_f$, increase and finally approach their asymptotic values; $\dot{m}''_f$ also increases with the external heat flux, $\dot{q}''_e$. Variations in the oxygen concentration of the environment also affect $\dot{q}''_{fr}$ and $\dot{m}''_f$. When the oxygen concentration in the environment is decreased below the ambient value, $\dot{m}''_f$ and $\dot{q}''_{fr}$ decrease until the flame extinction limit is reached. When the oxygen concentration in the environment is increased above the ambient value, $\dot{m}''_f$ and $\dot{q}''_{fr}$ increase until they reach their respective asymptotic values (oxygen concentration greater than about 30 percent with a material surface area of about 0.008 m^2).[3]

2.2.2 Fire chemistry. Fire chemistry is affected by fire ventilation. We define a ventilation parameter, ϕ, as

$$\phi = \dot{m}_a / \dot{m}_f \, k_a \, , \tag{13}$$

where k_a = theoretical mass of air consumed per unit mass of fuel vapors, also defined as the stoichiometric mass air-to-fuel ratio (g/g).

When $\phi > 1$, fires are defined as well ventilated and when $\phi < 1$, fires are defined as underventilated. From Eqs (1) and (13):

$$X_f = 1/(1 + k_a \, \phi) \, . \tag{14}$$

The parameters, H_i, χ_i, Y_j, f_j, and ξ_λ, are strong functions of the chemical structure of the material, as well as the decomposition processes followed by the material at various fire stages. In turbulent fires, these parameters are expected to be conserved for noncharring materials but vary with the extent of char formation, at various fire stages, for the char-forming materials.

2.2.3 Heat Losses. Values of ΔT are affected by heat losses. Laboratory-scale experiments can be designed such that heat losses are negligibly small. In enclosure fires, the heat losses could be quite significant, and, if the losses are not accounted for, then ΔT values would be in error.

Furthermore, in laboratory-scale experiments the distribution of $\dot{Q}_A$ into $\dot{Q}_C$ and $\dot{Q}_R$ can be quantified quite accurately, whereas in enclosure fires this distribution is not well defined. The distribution, however, can be defined in terms of the heat flow out of the enclosure, $\dot{Q}_g$, and heat lost within the enclosure, $\dot{Q}_\ell$. The relationship developed for $\dot{Q}_C$ and χ_C will still apply to $\dot{Q}_g$ and χ_g (combustion efficiency component associated with the temperature of the gas flowing out of the enclosure).

III EXPERIMENTS

Experiments were performed in three combustibility apparatuses: a 10-kW[1-7] scale, a 500-kW scale[8], and a 5000-kW scale apparatus[9].

In the apparatuses, the mass flow rate of the fuel vapors is monitored. The fire products are diluted and well mixed with ambient air as they are captured in the sampling ducts of each apparatus. The maximum flow rates of the mixture of fire products and air used in the 10-, 500-, and 5000-kW scale apparatuses are about 0.03, 2.0, and 28 m^3/s respectively. The measurements made in the sampling ducts include: total mass and volumetric flow rate of the mixture of fire products and air; gas temperature; light attenuation by particulates*; and concentration of CO_2, CO, hydrocarbons, and water*. The output from all the instruments is stored and analyzed by a computer.

IV RESULTS

4.1 Physical Similarity in Terms of Mass Flow Rate of Fuel Vapors from the Surface of the Material

The average steady state values of $\dot{m}''_f$, including the asymptotic values obtained by increasing either the surface area of the material or by increasing the oxygen concentration in the environment are listed in Table 1. A reasonable agreement can be noted between the asymptotic values of $\dot{m}''_f$ obtained by two different types of experiments. The data in Table 1 suggest that the fire scale effects on $\dot{m}''_f$ due to flame radiative heat flux can be compensated in the laboratory-scale fires by using either oxygen concentration in the environment greater than the ambient value or by using external heat flux.

4.2 Chemical Similarity in Terms of H_i, Y_j, and $\xi_\lambda Y_s$

The data for H_i, Y_j, and $\xi_\lambda Y_s$ are listed in Tables 2 and 3. An examination of the data indicates that, within the experimental variation of the data, there is a chemical similarity between various scale fires of each material under a specified mode of decomposition for well ventilated fires. For cellulosic material, flaming mode is defined as the initial fire stage, where flames are relatively taller; flaming/smoldering mode is defined as a mode which follows the initial flaming mode. In the flaming/smoldering mode, flames are relatively shorter accompanied by surface glowing; flames are intermittent and do not cover the entire surface of the material.

---

* not measured in the 5000-kW scale apparatus

TABLE 1. Average Steady State Values of the Mass Flow Rate of Fuel Vapors per Unit Surface Area of the Material[a]

Material	Surface Area (m^2)	$\dot{m}''_f$ ($g/m^2 s$) $X_O = 0.233$	$\dot{m}''_f$ ($g/m^2 s$) $X_O > 0.233$[b]
Pool-like Configuration			
Polyethylene/42% Chlorine	0.008	-	7
Polyvinyl Chloride	0.008	15	16
Polyoxymethylene	0.008	6	16
Methanol	0.008	16	20
	2.37	20[b]	-
Flexible polyurethane foams	0.008	-	21 to 27
Rigid polyurethane foams	0.008	-	22 to 25
Polypropylene	0.008	7	24
Polyethylene	0.008	8	26
High temp. hydrocarbon fluids	0.008	-	27 to 30
	2.37	25 to 29[b]	-
Polymethylmethacrylate	0.008	12	28
	2.37	30[b]	-
Polystyrene	0.008	14	38
	0.93	34[b]	-
Heptane	0.008	36	63
	1.17	66[b]	-
Three-Dimensional Arrangement			
Corrugated paper boxes	0.06[c]	9;14[e]	-
with shredded paper	53[d]	14	
Corrugated paper boxes	0.06[c]	14[e]	-
with a foam	53[d]	10	-
Pine wood cribs	0.26 to 11	8 to 11	-

[a] no external heat flux unless specified;

[b] asymptotic value;

[c] total exposed surface area of single box (0.1 x 0.1 x 0.1 m);

[d] total exposed surface area of sixteen boxes (four boxes on one pallet load, two pallet load wide x two pallet load deep x two tiers high, each box dimensions 0.53 x 0.53 x 0.53 m);

[e] 25 kW/m^2 of external heat flux on four sides.

For cellulosic materials, chemical similarity in terms of H_i and Y_{CO_2} is maintained for both flaming and flaming/smoldering modes. Chemical similarity in terms of Y_{CO} and $\xi_\lambda Y_S$, however, is maintained only if the decomposition mode does not change. For example, the average value of Y_{CO} = 0.0059 g/g in the flaming mode (except for cellulose and densely packed paper box) and 0.097 g/g for the flaming/smoldering mode. The average value of $\xi_\lambda Y_S$ in the flaming mode is 0.0075 m^2/g for cellulose and paper box and 0.078 m^2/g for oak, fir, and pine. In the flaming/smoldering mode, the average value of $\xi_\lambda Y_S$ = 0.67 m^2/g for paper box, 0.013 m^2/g for cellulose, and 0.15 m^2/g for pine-wood crib. In oxidative-pyrolysis, the average value of $\xi_\lambda Y_S$ = 0.80 m^2/g for oak and pine.

TABLE 2. Average Yields of CO_2, CO, and HCN and Heat of Combustion for Well Ventilated Fires of Materials in Pool-Like Configuration

Material	Surface Area (m^2)	Y_j (g/g)			H_1 (kJ/g)		
		CO_2	CO	HCN	Actual	Conv.	Rad.
Methanol	4.68	1.29	< 0.001	-	18.7	15.6	3.1
	2.32	1.30	< 0.001	-	18.8	15.7	3.1
	0.008	1.32	< 0.001	-	19.4	17.1	2.3
Rigid Polyurethane Foam	7	1.50	0.027	0.010	16.4	10.8	5.6
	0.008	1.51	0.036	0.012	15.8	6.5	9.3
Polymethylmethacrylate	2.37	2.11	0.008	-	24.2	15.8	8.4
	0.073	2.10	0.010	-	23.8	14.9	8.9
	0.008	2.15	0.011	-	24.4	17.9	6.5
High Temperature Hydrocarbon Fluids	2.37	-	-	-	35.6	23.8	11.8
	0.008	-	-	-	38.2	25.1	13.1
Heptane	0.92	2.83	0.015	-	41.2	26.8	14.4
	0.059	2.92	0.0090	-	42.5	26.2	16.3
	0.041	2.82	0.0081	-	40.9	26.9	14.0
	0.008	2.84	0.0091	-	40.8	24.8	16.0

4.3 Chemical Similarity in Terms of the Ratios of Generation Rates of Heat and Chemical Compounds, Light Attenuation by Particulates, and Depletion Rate of Oxygen

The generation of CO_2 and depletion of O_2 are associated with the generation of heat; an interrelationship between ΔT, X_{CO_2}, and X_O is thus expected:

$$\frac{(\Delta T/T_a)/(X_{CO_2} - X_{CO_2,a})}{(\Delta T/T_a)/(X_{Oa} - X_O)} = (k_O/k_{CO_2})\,(f_O/f_{CO_2}) \qquad (15)$$

where X_{CO_2} and X_O = measured mass fractions of CO_2 and O_2 respectively; $X_{CO_2,a}$ and X_{Oa} = measured ambient mass fractions of CO_2 and O_2 respectively; k_O and k_{CO_2} can be calculated from the measured elemental compositions of the materials. Chemical similarity in terms of f_O/f_{CO_2} thus can be established for various fire scales, irrespective of mixing and dilution of the compounds.

Our laboratory-scale data indicate that f_O/f_{CO_2} is conserved for numerous materials that we have examined, under a variety of experimental conditions, where $f_O = 0.98\ f_{CO_2}$. The data shown in Figure 1, for the enclosure fires of wood cribs under a variety of ventilation conditions, enclosure sizes, and crib sizes support our conclusion.

The data for f_O/f_{CO} indicate a strong dependency on the chemical structure of the material, decomposition chemistry, and fire ventilation; the effect of ventilation on this ratio is shown in Figure 2 for pine wood crib fires in enclosures and in our 10-kW scale apparatus. Data for cellulose and red oak have also been included in the figure. The data in Figure 2 indicate that f_O/f_{CO} is conserved for each value of X_f for various fire scales. With

TABLE 3. Average Yields of CO_2, CO, and Gaseous Hydrocarbons, Heat of Combustion, and Specific Extinction Coefficient for Well Ventilated Fires of Cellulosic Materials

Material	Configuration	Total Exposed Surface Area (m^2)	$\dot{q}''_e$ (kW/m^2)	Combustion Mode	H_i (kJ/g)			Y_j (kJ/g)			$\xi_\lambda Y_s$[b] (m^2/g)
					Actual	Conv.	Rad.	CO	CO_2	HC[a]	
Corrugated Paper	Box with sheets of paper (25% by weight)	0.06	0	Flaming	11.1	9.4	1.7	0.0082	1.12	c	0.0053
Corrugated Paper	Box with shredded paper (62% by weight)	0.06	0	Flaming	12.4	9.0	3.4	0.019	1.25	0.001	0.0067
				Flaming/Smold.	10.8	6.8	4.0	0.12	1.11	0.002	0.062
			10	Flaming	11.6	8.7	2.9	0.021	1.17	0.001	0.0067
				Flaming/Smold.	11.2	6.8	4.4	0.091	1.16	0.002	0.065
			21	Flaming	9.9	7.9	2.0	0.030	1.00	c	0.0062
				Flaming/Smold.	11.4	7.2	4.2	0.091	1.18	0.004	0.058
			31	Flaming	11.4	8.0	3.4	0.018	1.16	0.001	0.012
				Flaming/Smold.	11.8	7.8	4.0	0.110	1.27	0.021	0.082
Corrugated Paper	Boxes with shredded paper (19% by weight) on wood pallets (38% by weight)[d]	53	0	Flaming	12.3	9.2	3.1	0.0085	1.25	c	ND
Cellulose Powder	Pool	0.007	50	Flaming	12.8	9.1	3.7	0.0021	1.29	c	0.0057
Cellulose Filter Papers	Pool	0.007	50	Flaming/Smold.	10.2	5.8	4.3	0.095	1.05	0.001	0.013
Red Oak	Pool	0.007	31 to 71	Flaming	13.3	7.8	5.5	0.0039	1.34	c	0.086
				Oxid. Pyrolysis	NA	NA	NA	0.096	0.14	0.041	0.85
				Pyrolysis	NA	NA	NA	0.054	0.12	0.029	0.91
Douglas Fir	Pool	0.007	31 to 60	Flaming	13.0	8.1	4.9	0.0036	1.31	c	0.084
Pine	Wood-crib	0.062	0 to 60	Flaming	12.2	8.7	3.5	0.0054	1.31	c	0.064
				Flaming/Smold.	10.7	8.0	2.7	0.092	1.18	0.019	0.15
				Oxid. Pyrolysis	NA	NA	NA	0.18	0.23	0.060	0.68

[a] Total gaseous hydrocarbons

[b] $\lambda = 0.63\ \mu$

[c] < 0.001

[d] 16 boxes, four boxes on one pallet load; 2 pallets wide x 2 pallet loads deep x 2 tiers high ND not determined

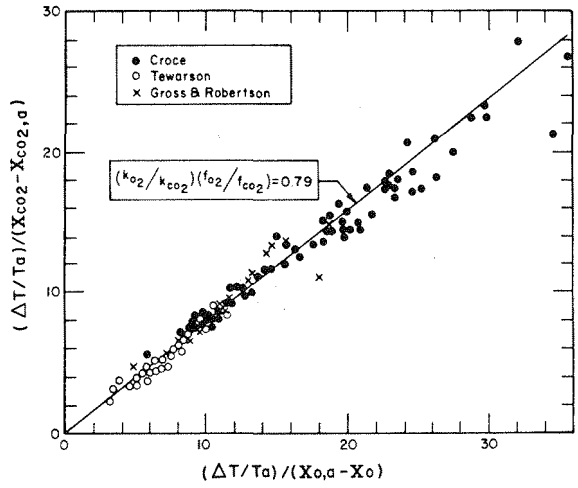

FIGURE 1. Chemical similarity in terms of the ratio of generation efficiency of CO_2 and depletion efficiency of O_2. Solid line is theoretical relationship. Experimental data taken from Refs. 10-12. Enclosure sizes from 0.21 to 22 m^3; exposed surface areas of cribs from 0.062 to 11 m^2.

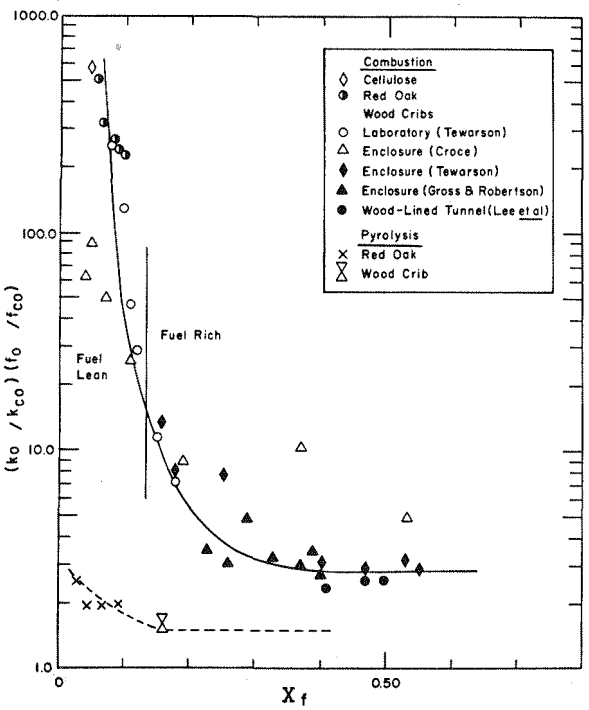

FIGURE 2. Dependency of the ratio of depletion efficiency of O_2 and generation efficiency of CO on fuel richness of the fire (Pyrolysis X_0 = 0.11).

increasing values of X_f (fire conditions changing from well ventilated to underventilated), f_O/f_{CO} approaches an asymptotic value (about 2.3 for combustion and about 1.2 for oxidative pyrolysis, for $X_f > 0.3$). If we assume $X_O = 0$, then the values of f_{CO} and Y_{CO} would be about 0.4 and 0.5 g/g in combustion and about 0.8 and 1.0 g/g in oxidative pyrolysis respectively. The maximum possible theoretical yield of CO for wood is 1.23 g/g.

The relationship between $\xi_\lambda Y_S$, and X_f is shown in Figure 3, where data for pine wood cribs from enclosure fires and from our 10-kW scale apparatus, together with cellulose and paper, have been included. The $\xi_\lambda Y_S$ values for paper products are lower than the value for pine wood crib under natural air flow. With increasing value of X_f, $\xi_\lambda Y_S$ values for red oak and pine wood crib increase, reaching a maximum value of about 0.12 m^2/g for 0.13 g/g < X_f > 0.20 g/g, indicating a maximum generation efficiency of particulates at this slightly fuel rich condition (for stoichiometric combustion of pine wood crib, X_f = 0.13 g/g.) For $X_f > 0.20$ g/g, in the enclosure fires of pine wood cribs, $\xi_\lambda Y_S$ decreases with increase in X_f, indicating a decrease in particulate formation. This suggests that the major fraction of the carbon in the fuel vapors is converted into the oxygenated species as X_f increases in the enclosure fires, which is in agreement with the conclusion derived previously[6] on the basis of the carbon atom balance.

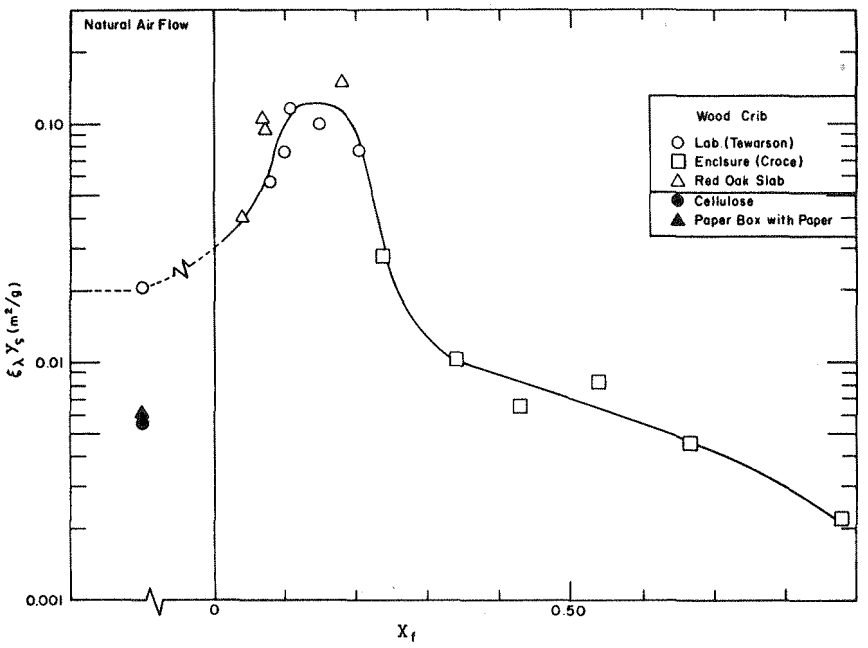

FIGURE 3. Dependency of the specific extinction coefficient of particulates on fuel richness of the fire.

V CONCLUSIONS

1. Experimental results obtained from the 10-, 500-, and 5000-kW scale apparatuses and enclosure fires of various sizes, for materials in pool-like, box-like and crib-like configurations, suggest that in turbulent fires of each material, under a specified value of the ventilation parameter and mode of decomposition, chemical similarity is maintained in terms of combustion efficiency and generation efficiency of chemical compounds and specific extinction coefficient of particulates.

2. The generation efficiency of CO and extinction coefficient of particulates was found to be very sensitive to the decomposition mode of cellulosic materials. The combustion efficiency and the generation efficiency of CO_2 was found to be less sensitive to the decomposition mode.

3. In the laboratory-scale experiments, it was possible to compensate the fire scale effects due to flame radiation by increasing the oxygen concentration in the environment above the ambient value.

4. The specific extinction coefficient of particulates for wood was found to reach a maximum value of about 0.12 m^2/g under slightly fuel-rich conditions.

5. The maximum possible yield of CO from wood fires was estimated to be about 0.5 g/g in combustion and about 1.0 g/g in oxidative pyrolysis.

ACKNOWLEDGEMENT

The financial support under Grant No. NB83NADA4021 from the U.S. National Bureau of Standards, Center for Fire Research, Washington, D.C. is deeply appreciated.

REFERENCES

1 Tewarson, A., "Physico-Chemical and Combustion Pyrolysis Properties of Polymeric Materials," National Bureau of Standards, Washington, D.C. NBS-GCR-80-295 (1980).

2 Tewarson, A., Flame Retardant Polymeric Materials, Volume 3, Lewin, Atlas and Pearce (editors). Plenum Press, New York, (1982).

3 Tewarson, A., Lee, J. L., and Pion, R. F., "The Influence of Oxygen Concentration on Fuel Parameters for Fire Modeling," Eighteenth Symposium (International) on Combustion, p. 563, The Combustion Institute (1980).

4 Tewarson, A.,"Quantification of Fire Properties of Fuels and Interaction with Fire Environment," National Bureau of Standards, Washington, D.C., FMRC J.I. OEON6.RC (1982).

5 Tewarson, A. and Steciak, J., "Fire Ventilation," Combustion and Flame, 53, (1983).

6 Tewarson, A., "Fully Developed Enclosure Fires of Wood Cribs," Twentieth Symposium (International) on Combustion. The Combustion Institute (in press).

[7] Tewarson, A., "Scale Effects on Fire Properties of Materials," National Bureau of Standards, Washington, D.C., FMRC J.I. 0J4N2.RC (1984).

[8] Newman, J. S., "Standard Test Criteria for Evaluation of Underground Fire Detection System," U.S. Bureau of Mines, Pittsburgh, PA, FMRC J.I. 0G2N4.RC (1984).

[9] Heskestad, G., "A Fire Products Collector for Calorimetry into the MW Range," Factory Mutual Research Corporation, Norwood, MA, FMRC J.I. 0C2E1.RA, June (1981).

[10] Gross, D. and Robertson, A. F., Experimental Fires in Enclosures," Tenth Symposium (International) on Combustion, p. 931, The Combustion Institute (1965).

[11] Tewarson, A., "Some Observations on Experimental Fires in Enclosures - Part I. Cellulosic Materials," Combustion and Flame, 19, 101 (1972).

[12] Croce, P. A., "Modeling of Vented Enclosures Fires, Part 1 - Quasi-Steady State Wood Crib Fire," Factory Mutual Research Corporation, Norwood, MA, FMRC J.I. 7A0R5.GU (1978).

[13] Lee, C. K., Chaiken, R. F., Singer, J. M. and Harris, M. E., "Behavior of Wood Fires in Model Tunnels under Forced Ventilation Flow," U. S. Bureau of Mines, Pittsburgh, PA, Report of Investigations 8450, 1980, available from Supt. of Docs. No. I28.23:8400.